

The Eurasia Proceedings of Science, Technology, Engineering and Mathematics (EPSTEM), 2025

Volume 38, Pages 47-55

**IConTES 2025: International Conference on Technology, Engineering and Science**

## **Development of High-Frequency Power Source Utilizing Electronic Ballast by Employing a Half-Bridge Inverter for Water Purification**

**Aicha Aissa-Bokhtache**

Hassiba Benbouali University of Chlef

**Maamar Latroch**

Hassiba Benbouali University of Chlef

**Taieb Bessaad**

Hassiba Benbouali University of Chlef

**Alla Eddine Toubal-Maamar**

University of Boumerdes

**Lemya Djafer**

Hassiba Benbouali University of Chlef

**Amina Merini**

Hassiba Benbouali University of Chlef

**Abstract:** This paper outlines the design of a high-frequency power supply, specifically an electronic ballast based *PWM* inverter, intended to power a low-pressure *UV* Mercury-Argon lamp. The lamp emits germicidal *UV* radiation at a wavelength of 253.7 nm, which effectively targets *DNA* viruses and bacteria present in the water to be treated. The system underwent thorough modeling, encompassing both the electronic ballast and the discharge lamp. The power supply employs a standard converter setup, comprising a half-bridge rectifier and inverter controlled by *PWM*. Simulations conducted using the MATLAB software environment yielded satisfactory results aligned with our objectives. The primary aim was to achieve a sinusoidal *rms* current precisely at 0.65 A, operating at a frequency of 50 kHz, to maximize *UVC* radiation at 253.7 nm. Hence, contemporary converters employing semiconductor switches operating at high-frequencies (over 50 kHz for MOSFETs) have been employed with proportional-integral control techniques.

**Keywords:** Low-pressure *UVC* Lamp, Germicide, Electronic ballast, *PWM* inverter, Half-bridge inverter, *PI* controller

### **Introduction**

In recent years, high-frequency electronic ballasts have emerged as a viable alternative to magnetic ballasts for discharge lamps due to their numerous advantages, including improved system performance (enhanced power factor), lightweight design, high luminous efficacy, long lifespan, lighting control capabilities, absence of flickering and audible noise (Aissa Bokhtache et al., 2024). However, it's crucial to carefully consider the cost implications associated with electronic ballasts (De Oro et al., 2014). During normal operation, discharge lamps exhibit negative differential resistance, necessitating effective current limiting mechanisms to prevent uncontrolled current growth. The presence of a ballast to regulate current is thus essential. The radiative characteristics of the lamp are influenced by factors such as gas mixture composition, discharge geometry, and

- This is an Open Access article distributed under the terms of the Creative Commons Attribution-Noncommercial 4.0 Unported License, permitting all non-commercial use, distribution, and reproduction in any medium, provided the original work is properly cited.

- Selection and peer-review under responsibility of the Organizing Committee of the Conference

electrical supply parameters like frequency and waveform. Key requirements for optimal operation include achieving zero average current, fast switching times, ensuring rapid re-ignition of the discharge at consistent currents, and the ability to operate as a cyclic current source with variable frequency.

## Description and Operating Principle of the System

Figure 1 shows the block diagram of the proposed system, Electronic ballast connected with half-bridge inverter. In this type of source, the inverter is configured as a high-frequency generator. The source consists of: A single-phase rectifier, The DC bus (link circuit), The transistor half-bridge inverter generating an output frequency of 50 kHz, A resonant circuit comprising  $L_r$  and  $C_r$  to facilitate lamp ignition, A filter is typically included between the main terminals and the rectifier to comply with electromagnetic compatibility (EMC) regulations and an additional preheating circuit is necessary to prevent filament damage. (Aissa Bokhtache et al., 2015).

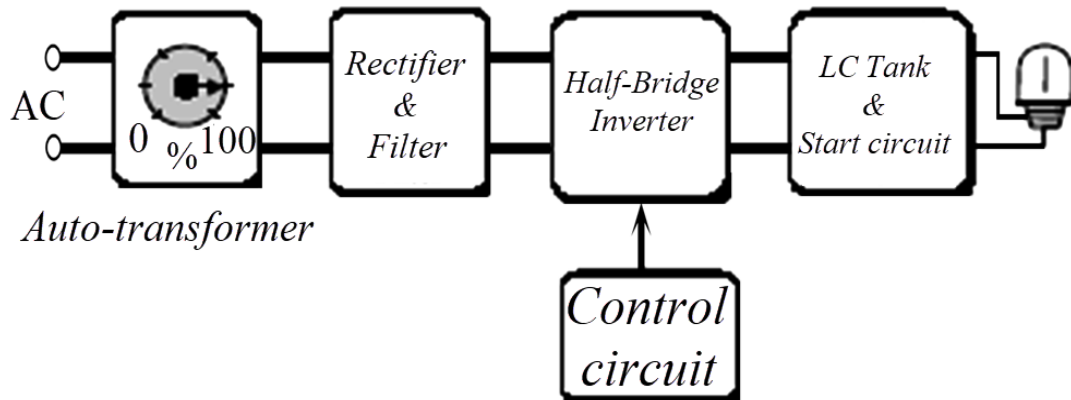


Figure 1. Block diagram of system consisting of a half-bridge inverter.

Figure 2 illustrates the electrical circuit of the proposed system.

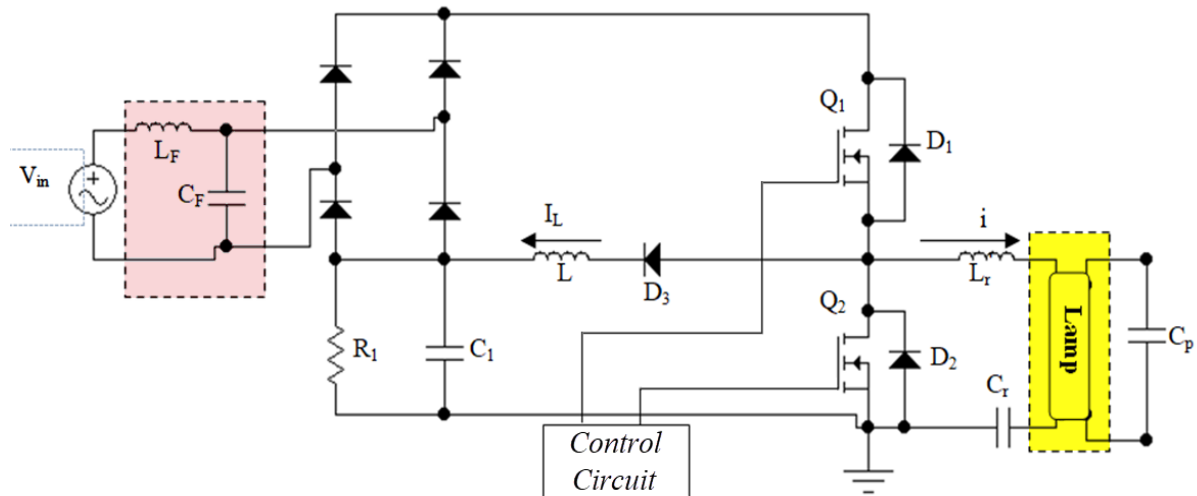


Figure 2. The electrical circuit of the proposed system.

The MOSFET is commonly employed in low-voltage applications with switching frequencies that can reach or exceed 100 kHz. It is also utilized for low-power applications. The operational principle of the proposed ballast's is described in steady-state modes, from mode 1 to mode 4. The equivalent circuit for each mode is depicted in Figure 3. To illustrate the circuit's equilibrium operation, all internal components are assumed to be ideal. This can be described as follows: (Aissa Bokhtache et al., 2016), (Kazufumi, et al., 2000).

**Mode 1:**  $t_0 < t < t_1$ : Between  $t_0$  and  $t_1$ : Prior to  $Q_1$  and  $Q_2$  entering their respective modes, both are in the off state. When  $Q_1$  is switched on at time  $t_0$ , a current flows through  $Q_1$  and is split into two components:  $i_{load}$  and  $i_L$ . The component  $i_L$  flows through  $D_3$ ,  $L$ , and  $C_1$ , while  $i_{load}$  flows through the fluorescent lamp.

**Mode 2:**  $t_1 < t < t_2$ : During Mode 2 ( $t_1 < t < t_2$ ): Following the turn-off of  $Q_1$  at  $t_1$  while  $Q_2$  remains off until  $t_2$ ,  $i_L$  flows through  $C_1$ ,  $D_2$ ,  $D_3$ ,  $L$ , and  $R$ , while  $i_{Load}$  flows through  $D_2$ ,  $L_r$ ,  $C_r$ , and the fluorescent lamp.

**Mode 3:**  $t_2 < t < t_3$ : At  $t_2$ ,  $Q_2$  is turned on.  $i_L$  reaches 0 between  $t_2$  and  $t_3$ . Subsequently, after  $i_{ch}$  reaches 0, it flows in the opposite direction compared to the operational state of  $Q_1$ , leading to a decrease in the negative peak.

**Mode 4:**  $t_3 < t < t_4$ : when stopped at  $t_3$   $Q_2$  and  $Q_1$  remains off status for the period from  $t_3$  to  $t_4$ ,  $t_4$   $i_L$  through  $D_3$ ,  $Q_1$  is on. The next mode is the mode 1.

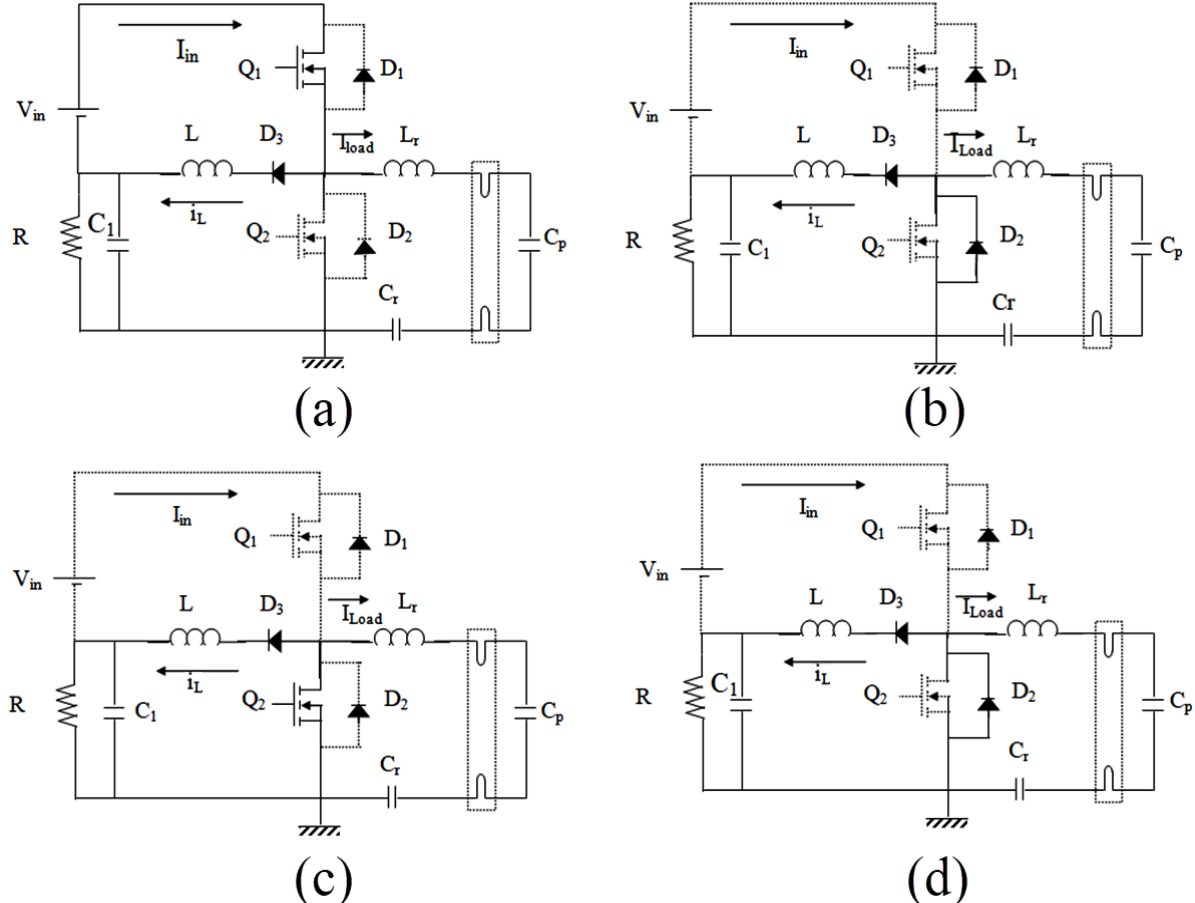


Figure 3. The equivalent circuits of the system operation modes.

### The Electrical Circuit Model of the Lamp

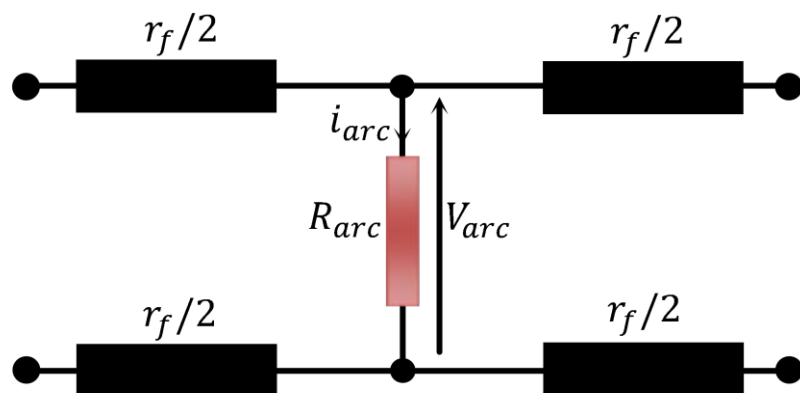


Figure 4. The fluorescent lamp electrical circuit model.

An electrical circuit model, depicted in Figure 4, has been proposed to characterize the electrical behavior of the fluorescent lamp when powered by a high-frequency electronic ballast. This model represents the lamp using two resistors:  $R_{arc}$ , which accounts for the electrical properties of the lamp's arc and is dependent on both power and temperature, and  $r_f$ , which represents the cathode filament (Aissa Bokhtache et al., 2017). Figure 5 illustrates the equivalent circuit of the system.

Where:

$$R_{arc} = \frac{V_{arc}}{i_{arc}} \quad (1)$$

$$P_{arc} = V_{arc} \cdot i_{arc} \quad (2)$$

With :  $R_{arc}$ : arc resistance,  $i_{arc}$ : arc current,  $V_{arc}$  :arc voltage,  $P_{arc}$  :arc power.

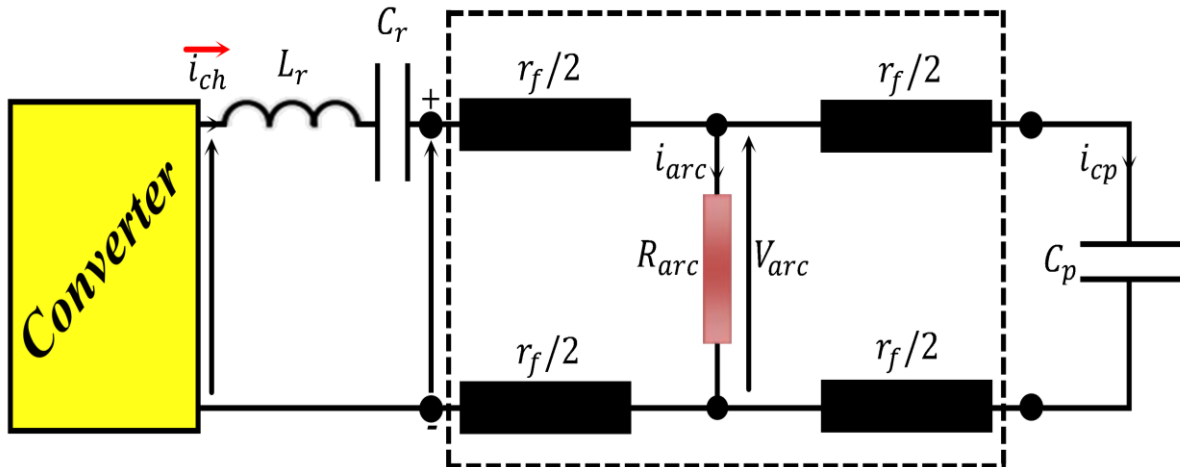


Figure 5. Equivalent circuit of the system.

The lamp voltage can be calculated as follows (7):

$$\begin{aligned} \vec{V}_{lamp} &= \vec{V}_{arc} + 2 \left[ \frac{r_f}{2} (\vec{i}_{arc} + \vec{i}_{Cp}) \right] = V_{arc} + i_{arc} r_f + \frac{r_f V_{arc}}{r_f - j Z_{Cp}} \\ &= \left[ \left( 1 + \frac{r_f^2}{r_f^2 + Z_{Cp}^2} \right) V_{arc} + r_f i_{arc} \right] + j \frac{r_f Z_{Cp}}{r_f^2 + Z_{Cp}^2} V_{arc} \end{aligned} \quad (3)$$

Therefore,

$$\vec{V}_{Lamp} = \left[ \left( 1 + \frac{r_f^2}{r_f^2 + Z_{Cp}^2} \right) V_{arc} + r_f \frac{P_{arc}}{V_{arc}} \right] + j \frac{r_f Z_{Cp}}{r_f^2 + Z_{Cp}^2} V_{arc} \quad (4)$$

With :  $Z_{Cp}$  is the reactance of the  $C_p$  capacitor and  $I_{Cp}$  is current which flows through it. The resonant load current is in fact the sum of both arc current and filament current. As a result, by calculating the transfer function of the open-loop system indicated in figure 5 we have:

$$\frac{I_{Load}}{V_{Load}} = \frac{(R_{arc} + r_f) C_r C_p S^2 + C_r S}{(R_{arc} + r_f) L_r C_r C_p S^3 [(2R_{arc} + r_f) L_r C_r C_p + L_r C_r] S^2 + (R_{arc} + r_f) (C_r + C_p) S + 1} \quad (5)$$

## Results and Discussion

The simulation results were conducted under the MATLAB/Simpower environment and are provided in the following figures. The converter frequency needs to be higher than the audible range, ensuring it operates effectively above 50 kHz. Additionally, the resonant circuit's resonant frequency is set at 42 kHz (Aissa Bokhtache et al., 2020; 2021).

Two tests are selected for comparison. The discharge lamp-electronic ballast system is first tested in an open-loop setup. Following this, the system is evaluated in a closed-loop arrangement using a traditional proportional-integral (PI) controller. The lamp used in the simulation is a real discharge lamp described in references (Aissa Bokhtache et al., 2023), the main characteristics of the discharge lamp-electronic ballast are given in (Table1) below:

Table 1. Characteristics of the discharge lamp-electronic ballast assembly.

Variables	Symbol	Values
Capacitance	$C_r$	$0.47 \mu F$
Capacitance	$C_P$	$3900 \mu F$
Inductance	$L_r$	$0.9 mH$
Power	$P_{Lamp}$	$65 W$
Frequency	$f$	$50 KHz$
Resistance	$R_{arc}$	$170.769 \Omega$
Resistance	$r_f$	$5 \Omega$
Voltage	$V_{in}$	$500V, 50Hz$
RMS Current	$I_{arc rms}$	$0.65 A$
Inductance	$L$	$1.27 mH$
Capacitance	$C_l$	$33 F$
Inductance	$L_F$	$1.5 mH$
Capacitance	$C_F$	$220 nF$

## Open-Loop Simulation Results

Figure 6 illustrates the obtained currents and voltages of the discharge lamp. Figure 7 resumes the THD of the arc voltage and the arc current of the discharge lamp. Figure 8 illustrates the waveform of the discharge lamp filament current, and Figure 9 shows the effective arc current of the discharge lamp.

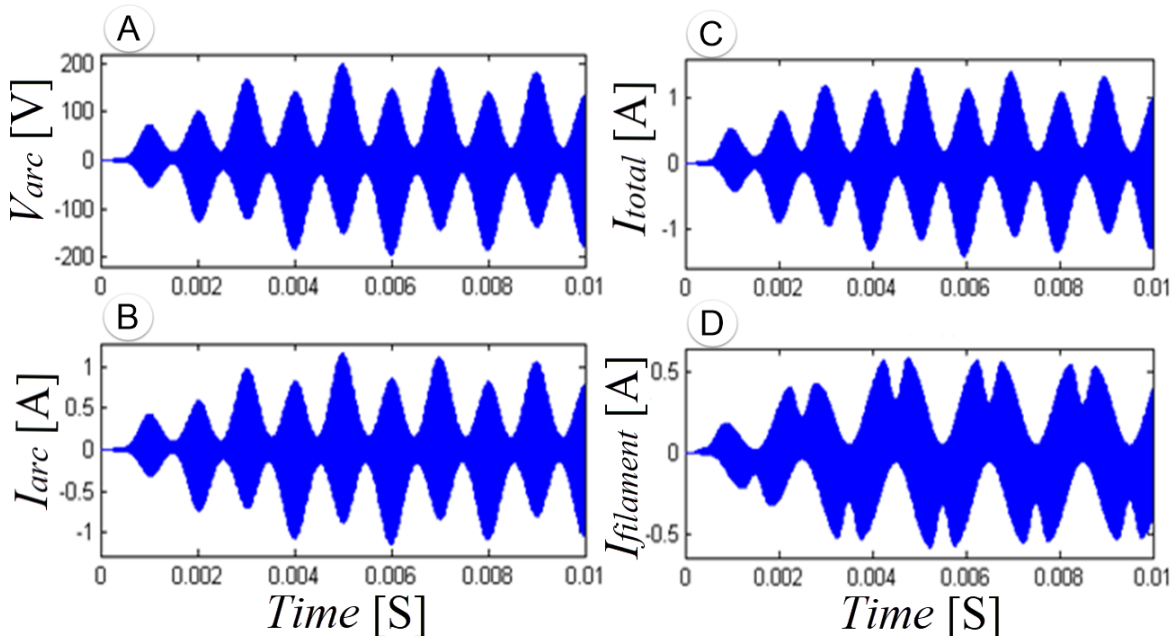


Figure 6. Curves of currents and voltages of the discharge lamp, (A) arc voltage, (B) arc current, (C) Total current and (D) filament current.

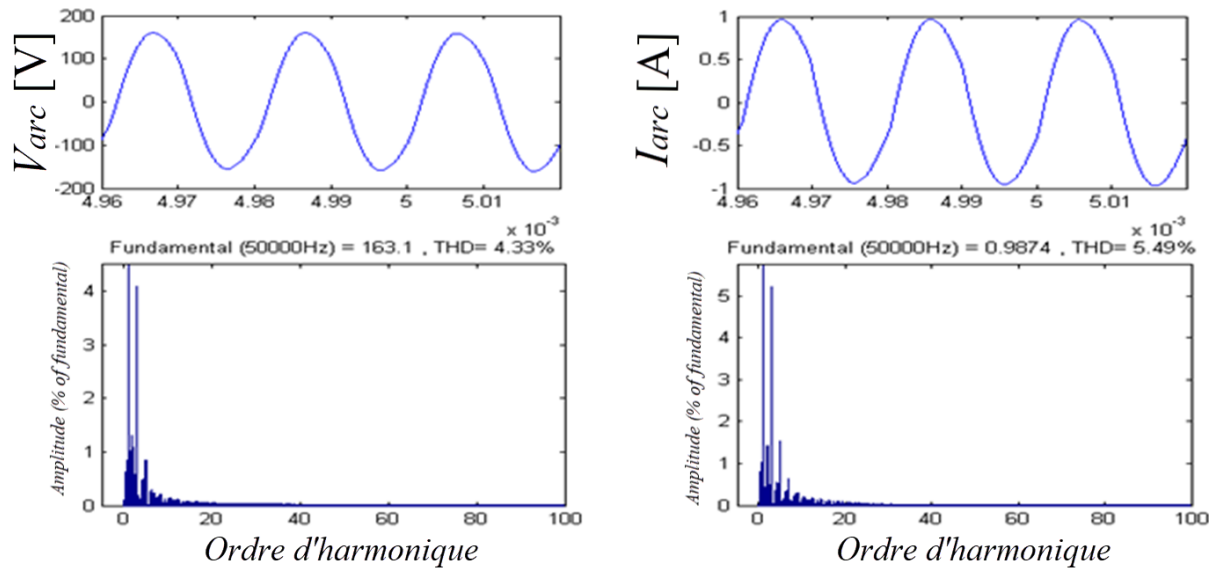


Figure 7. THD of the *arc* voltage and the *arc* current of the discharge lamp.

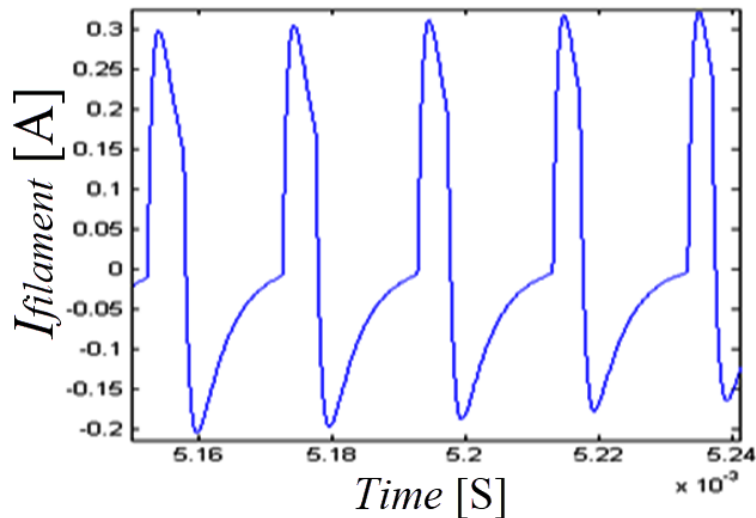


Figure 8. Waveform of the discharge lamp filament current.

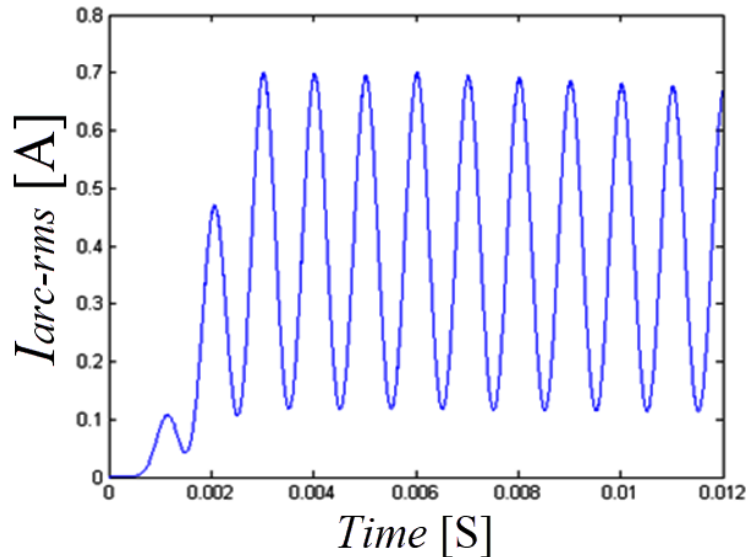


Figure 9. Effective *arc* current of the discharge lamp.

From figure 6, the obtained current and voltage exhibit sinusoidal waveforms, it can be observed that the voltage and current are modulated at a frequency of 50 kHz and contained in an envelope oscillating at 1 kHz with a modulation rate maximum/minimum values equal 5 approximately. From Figure 7, we can observe that the waveforms of current and voltage closely resemble sine waves, with *THD* values of 5.49 % for lamp *arc* current and 4.33 % for lamp voltage. The effective discharge lamp *arc* current varies as shown in Figure 9, indicating the need to regulate the current in our model to precisely achieve the targeted root mean square (*rms*) value of 0.65 A.

### Closed-Loop Simulation Results

To enhance the efficiency of water treatment and extend the lamp's lifespan, it is essential to operate the lamp with a constant root mean square (*rms*) value of the arc current. To meet this requirement, we initially investigated a closed-loop system incorporating a proportional-integral (*PI*) controller, commonly utilized in industrial applications. The closed-loop transfer function of the lamp-ballast system and its corresponding block diagram, implemented in the Matlab Sim-Power environment, are illustrated in Figure 10.

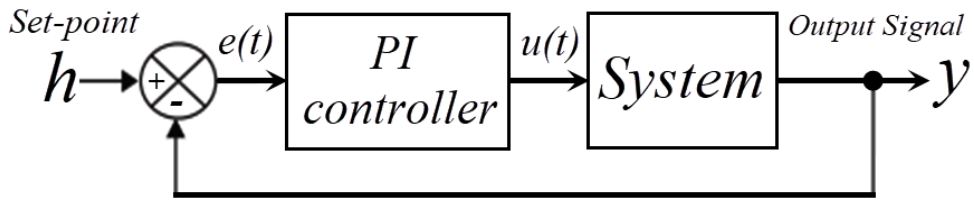


Figure 10. Closed-loop system with *PI* controller.

The simulation parameters were determined based on the lamp's characteristics and by solving the characteristic equation of the closed-loop transfer function using the pole placement method. The resulting simulation outcomes, including the time-domain behavior of the *arc* voltage, *arc* current, and its root mean square (*rms*) value, are presented in Figure 11.

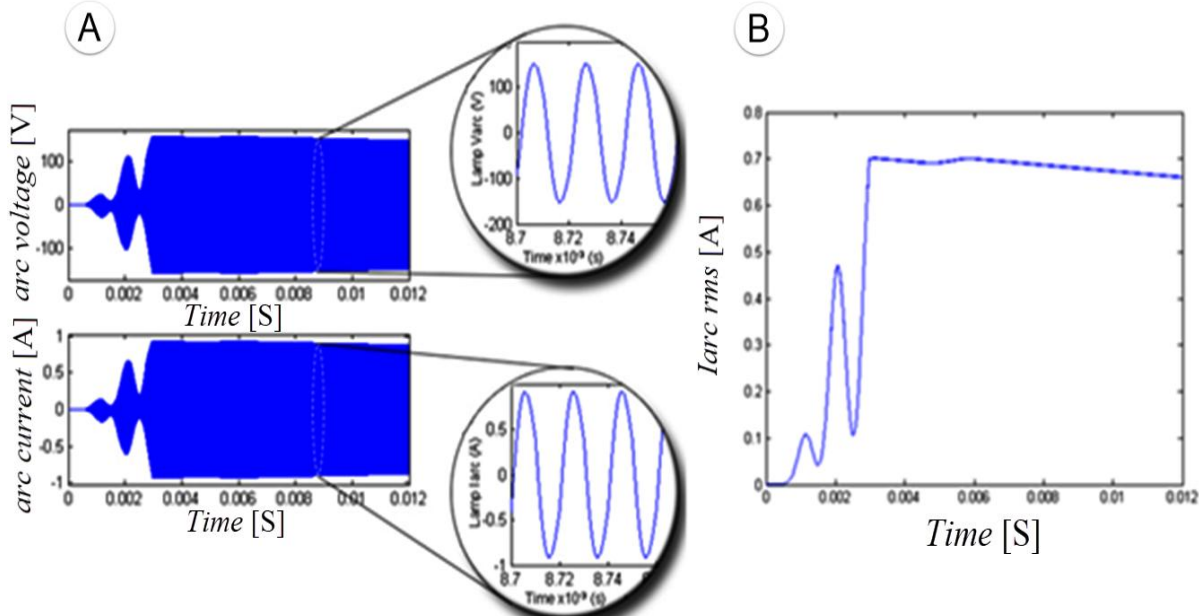


Figure 11. (a) Waveforms of the *arc* current and the *arc* voltage of the discharge lamp with a *PI* regulator. (b) *rms* value of the *arc* current of the discharge lamp after the application of a *PI*.

The analysis of the simulation results indicates that the control strategy employing a *PI* regulator exhibits a transient state similar to that of the open-loop controller. However, in steady state, it demonstrates excellent static and dynamic performance, with a current frequency of 50 kHz and a constant root-mean-square (*rms*) value of 0.65A, aligning with the desired values that optimize the germicidal effect.

## Conclusion

The implementation of discharge lamps in industrial applications requires interdisciplinary knowledge, including electrical engineering, optics, plasma physics, and chemistry. We have established the foundational aspects of our study on the power of discharge lamps with electronic ballasts. The first part focused on presenting the general structure of an electronic ballast, utilizing a half-bridge inverter, selecting switches and their characteristics, modeling the electrical circuit of the fluorescent lamp, and assessing the relative influences of various parameters of the electronic components comprising the electronic ballast. The electrical behavior of the fluorescent lamp, powered by a high-frequency electronic ballast, can be represented by a power-dependent resistor and temperature. The second part of this study involved MATLAB simulation of the electronic ballast circuit. Although the current and voltage waveforms closely resembled a sine wave (with a total harmonic distortion of 5.49 % for current and 4.33 % for voltage) at a frequency of 50 kHz, we encountered challenges in achieving a consistent current of 0.65 A. The implementation of a feedback loop with a PI controller eliminates the oscillations in the effective current and enables the system to stabilize around the desired value of 0.65 A.

## Scientific Ethics Declaration

\* The authors declare that the scientific ethical and legal responsibility of this article published in EPSTEM journal belongs to the authors.

## Conflict of Interest

\* The authors declare that they have no conflicts of interest.

## Funding

\* This work was supported in part by the Faculty of Technology, Hassiba Benbouali University of Chlef; in part by the Faculty of Technology, University of M'hamed Bougara of Boumerdes, and the Directorate-General for Scientific Research and Technological Development (DGRSDT), Algeria.

## Acknowledgements or Notes

\* This article was presented as an oral presentation at the International Conference on Technology, Engineering and Science ([www.icontes.net](http://www.icontes.net)) held in Antalya/Türkiye on November 12-15, 2025.

## References

Aissa-Bokhtache, A., Latroch, M., Badni, N., Toubal Maamar, A. E., Djafer, L., & Merini, A. (2024). Comparative analysis of three converters providing power to a discharge lamp-electronic ballast system designed for water sterilization. *The Eurasia Proceedings of Science, Technology, Engineering & Mathematics (EPSTEM)*, 32, 53–65.

Aissa-Bokhtache, A., Latroch, M., Toualbia, A., Djafer, L., & Benallou, M. (2023). Modern control of a power supply based on a matrix converter for water disinfection by UVC radiation. *The Eurasia Proceedings of Science, Technology, Engineering & Mathematics (EPSTEM)*, 26, 733–740.

Aissa-Bokhtache, A., Latroch, M., Toualbia, A., Toubal Maamar, A. E., & Boucherit, M. S. (2023). Optimization of a power supply using 3 types of converters of a discharge lamp-electronic ballast system for water purification. *Proceedings of 2nd International Conference on Electronics, Energy and Measurement (IC2EM)*, 1–6.

Aissa-Bokhtache, A., Zegaouia, A., Taleb, R., & Aillerie, M. (2021). Control of an electronic ballast-discharge lamp system supplied by a multicellular converter dedicated to water purification. *Desalination and Water Treatment*, 228, 176–186.

Aissa-Bokhtache, A., Zegaoui, A., Aillerie, M., Djahbar, A., Allouache, H., Hemici, K., Kessassia, F. Z., & Bouchrit, M. S. (2017). Power supply improvements for ballasts-low pressure mercury/argon discharge lamp for water purification. *AIP Conference Proceedings*, 1814, 020059.

Aissa-Bokhtache, A., Zegaoui, A., Belmadani, B., & Bouchrit, M. S. (2015). Water purification by a lamp discharge-electronic ballast system using a full bridge inverter. *Energy Procedia*, 74, 446–452.

Aissa-Bokhtache, A., Zegaoui, A., Kellal, M., Boucherit, M. S., Belmadani, B., & Aillerie, M. (2016). Optimization based on fuzzy logic control of discharge lamp-electronic ballast system for water purification. *Electric Power Components and Systems*, 44, 1981–1990.

Aissa-Bokhtache, A., Zegaoui, A., Taleb, R., & Aillerie, M. (2020). Super twisting sliding mode control algorithm of a discharge lamp for water sterilization. *Kansai University Reports*, 62(04), 1731–1741.

Cheng, C. A., Cheng, H. L., Chu, K. L., & Lin, K. J. (2010). A constant power controller of DC-AC electronic ballast inverter for HID lamps. *The 2010 International Power Electronics Conference - ECCE ASIA* -, 414–419.

Costache, M. C., Damelincourt, J. J., & Zissis, G. (2000). Optimisation of an ultraviolet source working in a consumer water reactor. *UVX 2000: Colloque sur les Sources Cohérentes et Incohérentes UV, VUV, et X – Applications et Développements Récents*, 87(5), 65–66.

De Oro, L. A., Melo, G. A., & Canesin, C. A. (2014). UV dose investigation for immersed lamp purifier for electronic ballast UV lamps design. *IEEE 16th International Power Electronics and Motion Control Conference and Exposition (PEMC)*, 893–900.

Takagi, K., Jinno, M., & Aono, M. (2000). The study of electronic ballast for fluorescent lamp with an electronic device given two functions. *Conference Record of the 2000 IEEE Industry Applications Conference. Thirty-Fifth IAS Annual Meeting and World Conference on Industrial Applications of Electrical Energy*, 5, 3382–3387.

Vijayakumar, K., & Rajan, S. E. (2011). Performance evaluation of inverter topology employing controlled-capacitor-charging technique. *2011 International Conference on Emerging Trends in Electrical and Computer Technology*, 398–406.

---

### Author(s) Information

---

**Aicha Aissa-Bokhtache**

Hassiba Benbouali University of Chlef, Laboratoire Génie Electrique et Energies Renouvelables (LGEER), Faculty of Technology, Electrical Engineering Department, BP. 151, Hai Essalam, 02000 Chlef, Algeria.  
Contact e-mail: [ahcial71@gmail.com](mailto:ahcial71@gmail.com)

**Maamar Latroch**

Hassiba Benbouali University of Chlef, Laboratoire Génie Electrique et Energies Renouvelables (LGEER), Faculty of Technology, Electrical Engineering Department, BP. 151, Hai Essalam, 02000 Chlef, Algeria.

**Taieb Bessaad**

Hassiba Benbouali University of Chlef, Laboratoire Génie Electrique et Energies Renouvelables (LGEER), Faculty of Technology, Electrical Engineering Department, BP. 151, Hai Essalam, 02000 Chlef, Algeria.

**Alla Eddine Toubal-Maamar**

University of Boumerdes (University of M'Hamed Bougara of Boumerdes), Department of Electrical Systems Engineering, Faculty of Technology, Laboratoire Ingénierie des Systèmes et Télécommunications (LIST), Frantz Fanon city, 35000 Boumerdes, Algeria.

**Lemya Djafer**

Hassiba Benbouali University of Chlef, Laboratoire Génie Electrique et Energies Renouvelables (LGEER), Faculty of Technology, Electrical Engineering Department, BP. 151, Hai Essalam, 02000 Chlef, Algeria.

**Amina Merini**

Hassiba Benbouali University of Chlef, Laboratoire Génie Electrique et Energies Renouvelables (LGEER), Faculty of Technology, Electrical Engineering Department, BP. 151, Hai Essalam, 02000 Chlef, Algeria

---

**To cite this article:**

Aissa-Bokhtache, A., Latroch, M., Bessaad, T., Toubal-Maamar, A.E., Djafer, L. & Merini, A (2025). Development of high-frequency power source utilizing electronic ballast by employing a half-bridge inverter for water purification. *The Eurasia Proceedings of Science, Technology, Engineering and Mathematics (EPSTEM)* ,38, 47-55